Nickel Thioether Chemistry: a Re-examination of the Electrochemistry of $[Ni([9]aneS_3)_2]^{2+}$. The Single-crystal X-Ray Structure of a Nickel(III) Thioether Complex, $[Ni^{III}([9]aneS_3)_2][H_5O_2]_3[ClO_4]_6$ ($[9]aneS_3$ = 1,4,7-trithiacyclononane)†

Alexander J. Blake, Robert O. Gould, Malcolm A. Halcrow, Alan J. Holder, Timothy I. Hyde and Martin Schröder*
Department of Chemistry, The University of Edinburgh, West Mains Road, Edinburgh EH9 3JJ, UK

Cyclic voltammetry of $[Ni([9]aneS_3)_2][PF_6]_2$ ($[9]aneS_3$ = 1,4,7-trithiacyclononane) in MeCN (0.1 mol dm^{-3} NBu_4PF_6) at 293 K at platinum electrodes shows the previously reported chemically reversible oxidation at $E_{\frac{1}{2}} = +0.98$ V, $\Delta E_p = 82$ mV and a quasi-reversible reduction at $E_{\frac{1}{2}} = -1.11$ V *vs.* ferrocene–ferrocenium, $\Delta E_p = 90$ mV. These redox processes have been investigated spectroelectrochemically using ESR and electronic spectroscopy which indicate $[Ni([9]aneS_3)_2]^{3+}$ to be a genuine d^7 nickel(III) complex. The $[Ni([9]aneS_3)_2]^{3+}$ cation can be generated quantitatively and stabilised for extended periods by dissolution of $[Ni([9]aneS_3)_2]^{2+}$ in $HClO_4$ solution. The complex $[Ni^{III}([9]aneS_3)_2][H_5O_2]_3[ClO_4]_6$ crystallises in the rhombohedral space group $R\bar{3}c$. The single-crystal X-ray structure confirms octahedral homoleptic thioether co-ordination with Ni–S bond lengths of 2.3129(25) Å. These Ni–S distances are significantly shorter than in the nickel(II) analogue $[Ni([9]aneS_3)_2]^{2+}$ and confirm the formulation of a mononuclear nickel(III)–thioether complex cation. Cyclic voltammetry of $[Zn([9]aneS_3)_2][PF_6]_2$ reveals one irreversible oxidation and one irreversible reduction at $E_{pa} = +1.30$ and $E_{pc} = -1.77$ V respectively at a scan rate of 400 mV s^{-1}. Significantly, the redox potential for the oxidation of the zinc(II) species is more anodic than for the nickel(II) analogue.

The discovery of redox-active nickel centres in sulfur-rich environments in nickel hydrogenase and CO oxido-reductase enzymes[1] has led to intense interest in the redox chemistry of nickel complexes of thiolate and thioether ligands.[2–4] Electrochemical or chemical oxidation of nickel thiolate complexes can result in oxidation of the thiolate ligands to disulfides.[2] However, it has been shown recently that the unusually cathodic Ni^{II}–Ni^{III} oxidation potentials observed in several hydrogenase enzymes can be reproduced in nickel complexes of constrained polythiolate or mixed amine–thiolate donor ligands.[3] We were, therefore, interested in the redox chemistry of nickel complexes containing a homoleptic hexathia co-ordination sphere such as $[Ni([9]aneS_3)_2]^{n+}$ ($[9]aneS_3$ = 1,4,7-trithiacyclononane **1**).[5]

The cyclic voltammogram of the homoleptic hexathia complex $[Ni([9]aneS_3)_2]^{2+}$ was first reported by Wieghardt *et al.*,[6] who described a chemically reversible oxidation at $E_{\frac{1}{2}} = +0.97$ V *vs.* ferrocene–ferrocenium. This oxidative couple was not characterised further, although the oxidation product was tentatively formulated as a nickel(II)-stabilised ligand-radical cation $[Ni^{II}([9]aneS_3)([9]aneS_3^{+})]^{3+}$ on the grounds that the above oxidation potential is similar to that exhibited by free $[9]aneS_3$ under similar conditions ($E_{pa} = +0.99$ V). During the course of our own synthetic, structural and electrochemical studies of polythia macrocyclic complexes[7] we have shown $[9]aneS_3$ to form unusually stable bis(sandwich) complexes $[M([9]aneS_3)_2]^{n+}$ of the d^7 metal ions Pd^{III},[8,9] Pt^{III}[10] and Rh^{II}.[9,11] We have also recently shown that the electrochemical or chemical oxidation of $[9]aneS_3$ under anaerobic conditions leads to the formation of a bicyclic sulfonium cation **2**,[12] which we argued was unlikely to occur on oxidation of a facially co-ordinated $[9]aneS_3$ ligand. Therefore, a re-investigation of the electrochemistry of $[Ni([9]aneS_3)_2]^{2+}$ was undertaken, with the aim of characterising unambiguously the redox products thus generated.

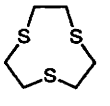
$[9]aneS_3$ **1**

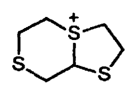
2

Results and Discussion

The complex $[Ni([9]aneS_3)_2][PF_6]_2$ was prepared according to literature methods.[5,6] The cyclic voltammogram of $[Ni([9]aneS_3)_2][PF_6]_2$ in MeCN (0.1 mol dm^{-3} NBu_4PF_6) at 293 K exhibited a chemically reversible oxidation at platinum electrodes at $E_{\frac{1}{2}} = +0.98$ V *vs.* ferrocene–ferrocenium, ΔE_p = 82 mV (scan rate 400 mV s^{-1}) close to the previously reported potential. Coulometric measurements on the oxidation of $[Ni([9]aneS_3)_2]^{2+}$ in MeCN containing 0.1 mol dm^{-3} NBu_4PF_6 at 253 K[6] confirmed the process to be essentially a one-electron process, the value of *n* being typically 0.94 electrons per Ni. A *quasi*-reversible reduction was also observed at $E_{\frac{1}{2}} = -1.11$ V, ΔE_p = 90 mV, which became chemically reversible at 253 K.

Controlled-potential electrolysis of $[Ni([9]aneS_3)_2][PF_6]_2$ in MeCN containing 0.1 mol dm^{-3} NBu_4PF_6 at +1.20 V *vs.* ferrocene–ferrocenium at 253 K affords orange-red solutions of $[Ni([9]aneS_3)_2]^{3+}$, the ESR spectrum of which, recorded as a frozen MeCN glass at 77 K, exhibits a rhombic spectrum with

---

† *Supplementary data available:* see Instructions for Authors, *J. Chem. Soc., Dalton Trans.*, 1992, Issue 1, pp. xx–xxv.

Non-SI unit employed: G = 10^{-4} T.

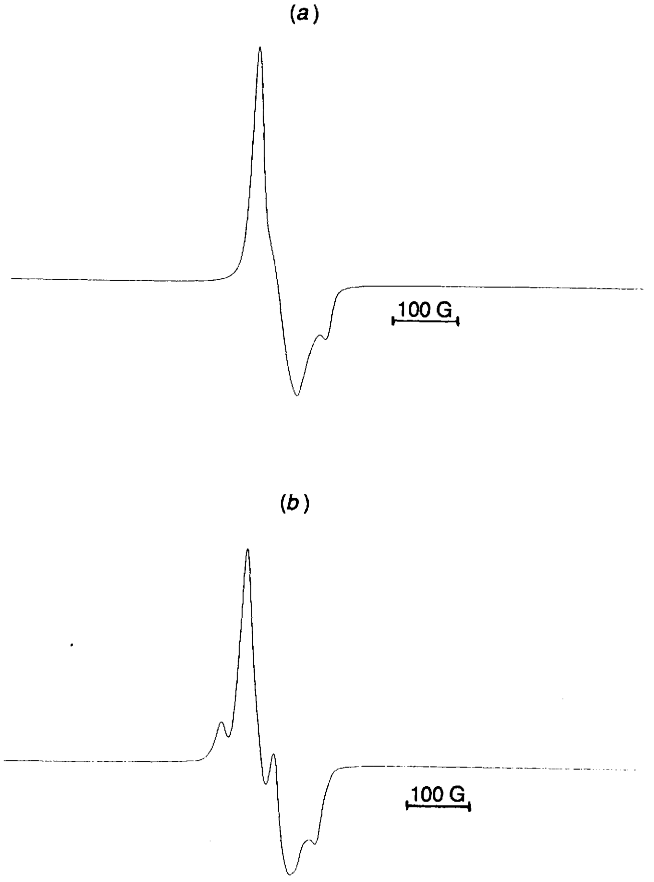

Fig. 1 X-Band ESR spectrum of $[Ni([9]aneS_3)_2]^{3+}$ in MeCN (0.1 mol dm^{-3} NBu_4PF_6) at 77 K; (*a*) unenriched sample, (*b*) enriched sample with 62% ^{61}Ni ($I = \frac{3}{2}$)

$g_1 = 2.093$, $g_2 = 2.075$, $g_3 = 2.027$ (Fig. 1) and at 293 K as a fluid solution, $g_{iso} = 2.065$. Deep orange-red solutions of $[Ni([9]aneS_3)_2]^{3+}$ can also be generated chemically by dissolution of $[Ni([9]aneS_3)_2][PF_6]_2$ in 70% $HClO_4$ or 98% H_2SO_4: these solutions show similar ESR spectra to those of the electrogenerated samples ($g_1 = 2.094$, g_2 unresolved, $g_3 = 2.025$ in 70% $HClO_4$ at 77 K), although the products generated chemically under acidic conditions are more stable than the electrogenerated solutions. Acidic solutions of the chemically-oxidised complex are stable indefinitely (over several weeks) whereas electrogenerated solutions in MeCN with 0.1 mol dm^{-3} NBu_4PF_6 decompose slowly over a period of 2 h. The g values for the oxidation product of $[Ni([9]aneS_3)_2][PF_6]_2$ are similar to those reported for other octahedral complexes of nickel(III),[13] including the related species $[Ni([9]aneN_3)_2]^{3+}$ ($g_\perp = 2.127$, $g_\parallel = 2.030$)[14,15] and $[Ni([9]aneNS_2)_2]^{3+}$ ($g_\perp = 2.121$, $g_\parallel = 2.019$)[16] ($[9]aneN_3$ = 1,4,7-triazacyclononane, $[9]aneNS_2$ = 1,4-dithia-7-azacyclononane). The pattern of $g_\perp > g_\parallel$ observed for these and other octahedral nickel(III) complexes is consistent with a d_{z^2} electronic ground state.

In order to confirm the metal-centred character of $[Ni([9]aneS_3)_2]^{3+}$, a sample of 62% ^{61}Ni-enriched $[Ni([9]aneS_3)_2]^{3+}$ was prepared by chemical and electrochemical oxidation of an enriched sample of $[Ni([9]aneS_3)_2]^{2+}$. The ESR spectrum of 62% ^{61}Ni-enriched $[Ni([9]aneS_3)_2]^{3+}$ at 77 K in MeCN glass containing 0.1 mol dm^{-3} NBu_4PF_6 (Fig. 1) exhibits two well resolved components of hyperfine coupling to ^{61}Ni ($I = \frac{3}{2}$), $A_1 = 28$ G and $A_3 = 7$ G, the latter component being obtained from the second derivative spectrum. The solution X-band ESR spectrum of $[^{61}Ni([9]aneS_3)_2]^{3+}$ at 293 K shows a slightly broadened singlet resonance at $g_{iso} = 2.065$, with A_{iso} (^{61}Ni) not resolved. The same spectrum is obtained by chemical oxidation of the enriched $[Ni([9]aneS_3)_2]^{2+}$ with $HClO_4$. For an $S = \frac{1}{2}$ radical with a d_{z^2} ground state, consideration of metal–ligand σ bonding leads to the following expressions for hyperfine coupling to the metal nucleus [equations (1) and (2)],[17]

$$A_\perp = -K + P_0[(\tfrac{2}{7})\alpha^2 - \tfrac{15}{14}(g_\perp - g_e)] \qquad (1)$$

$$A_\parallel = -K + P_0[(\tfrac{4}{7})\alpha^2 - \tfrac{1}{7}(g_\perp - g_e)] \qquad (2)$$

where K is the Fermi contact term for isotropic hyperfine coupling to the metal nucleus, P_0 is the coupling constant for dipole–dipole coupling to the free metal ion ($P_0 = 102$ G for ^{61}Ni)[18] and α^2 is a covalency factor that gives the reduction in the observed dipole–dipole coupling constant from the free-ion term P_0. Solution of the above equations using the g, A_1 and A_3 values derived from the ESR spectrum of $[^{61}Ni([9]aneS_3)_2]^{3+}$ affords the covalency factors $\alpha^2 = 0.39$ for $A_1 = +28$ G, $A_3 = +7$ G, or $\alpha^2 = 0.56$ for $A_1 = +28$ G, $A_3 = -7$ G. Both these solutions must be considered, because the relative signs of A_1 and A_3 cannot be deduced from the isotropic ESR spectrum of the enriched cation. Very little ^{61}Ni ESR data have been reported for nickel(III) complexes. Nickel-61 hyperfine coupling constants have been published for several oxidised nickel 1,2-dithiolene complexes, giving $\alpha^2 \approx 0.20$,[19] which has led to these species being formulated as nickel(II)-stabilised ligand-radical cations. A similar analysis of *trans*-$[^{61}Ni(phmp)_2Cl_2]^+$ [phmp = *o*-phenylenebis(dimethylphosphine) afforded a covalency factor of 0.42 for this complex, which was therefore assigned as a metal-based radical.[20] Hence, both possible α^2 values for $[Ni([9]aneS_3)_2]^{3+}$ imply a degree of metal character consistent with a genuine d^7 nickel(III) complex. Clearly, there remains ambiguity as to the precise degree of metal character in the radical product. Most notably, the above approach neglects π bonding in the complex: this may be significant with relatively soft, polarisable donors such as thioethers. We therefore set out to obtain a single-crystal X-ray structure of the oxidised complex $[Ni([9]aneS_3)_2]^{3+}$ which would allow us to distinguish between a metal- or ligand-based radical species.

The oxidation of $[Ni([9]aneS_3)_2]^{2+}$ was monitored spectroelectrochemically at reduced temperatures using an optically transparent electrode system. Fig. 2 shows the changes in the electronic spectrum on oxidation of $[Ni([9]aneS_3)_2]^{2+}$ to $[Ni([9]aneS_3)_2]^{3+}$ at $+1.20$ V at 253 K in MeCN containing 0.1 mol dm^{-3} NBu_4PF_6. Importantly, the oxidation occurs isosbestically, $\lambda_{iso} = 338$ and 290 nm, with collapse of the S→Ni charge-transfer band of the nickel(II) precursor at $\lambda_{max} = 319$ nm, $\varepsilon_{max} = 16\,180$ dm^3 mol^{-1} cm^{-1}, and concomitant growth of two new sets of charge-transfer absorptions at lower energy, $\lambda_{max} = 492$, 428 and 387 nm, $\varepsilon_{max} = 4620$ (sh), 11 005 (sh) and 13 870 dm^3 mol^{-1} cm^{-1}, and at $\lambda_{max} = 326$, 271 and 235 nm, $\varepsilon_{max} = 3280$, 6035 (sh) and 9900 dm^3 mol^{-1} cm^{-1}. Re-reduction of the oxidised complex results in quantitative regeneration of $[Ni([9]aneS_3)_2]^{2+}$. At temperatures higher than 260 K, loss of isosbesticity in the redox interconversion is observed, consistent with the relative instability of the oxidation product.

Attempts to grow single crystals containing $[Ni([9]aneS_3)_2]^{3+}$ from organic solvents failed. This was partly due to the relative instability of the 3+ cation in such media. We have previously shown that 3+ cations of the type $[M([9]aneS_3)_2]^{3+}$ (M = Pd, Pt or Au) can be stabilised under acidic conditions,[7] thereby inhibiting a competing ring-opening reaction to form a vinyl–thioether species.[21] Under acidic conditions ($HClO_4$ or H_2SO_4) $[Ni([9]aneS_3)_2]^{3+}$ is indeed stable. Single crystals of $[Ni([9]aneS_3)_2][H_5O_2]_3[ClO_4]_6$ were obtained by recrystallisation of $[Ni([9]aneS_3)_2][PF_6]_2$ from 70% $HClO_4$. The single-crystal X-ray structure of this complex shows (Fig. 3) the Ni centre on a site of $\bar{3}$ crystallographic symmetry and surrounded by an octahedron of six thioether donors. All six Ni–S bond lengths are constrained by symmetry to have the same value of 2.3129(25) Å, significantly shorter than those observed for $[Ni([9]aneS_3)_2]^{2+}$, Ni–S = 2.377(1), 2.381(1), 2.400(1) Å.[5]

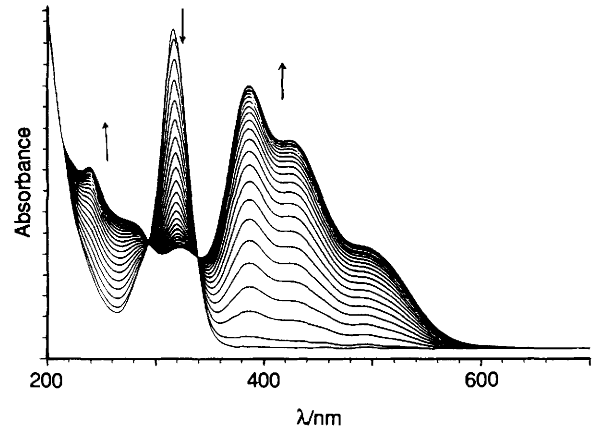

Fig. 2 Oxidation of $[Ni([9]aneS_3)_2]^{2+}$ by controlled-potential electrolysis at +1.20 V *vs.* ferrocene–ferrocenium in MeCN (0.1 mol dm^{-3} NBu_4PF_6) at 253 K

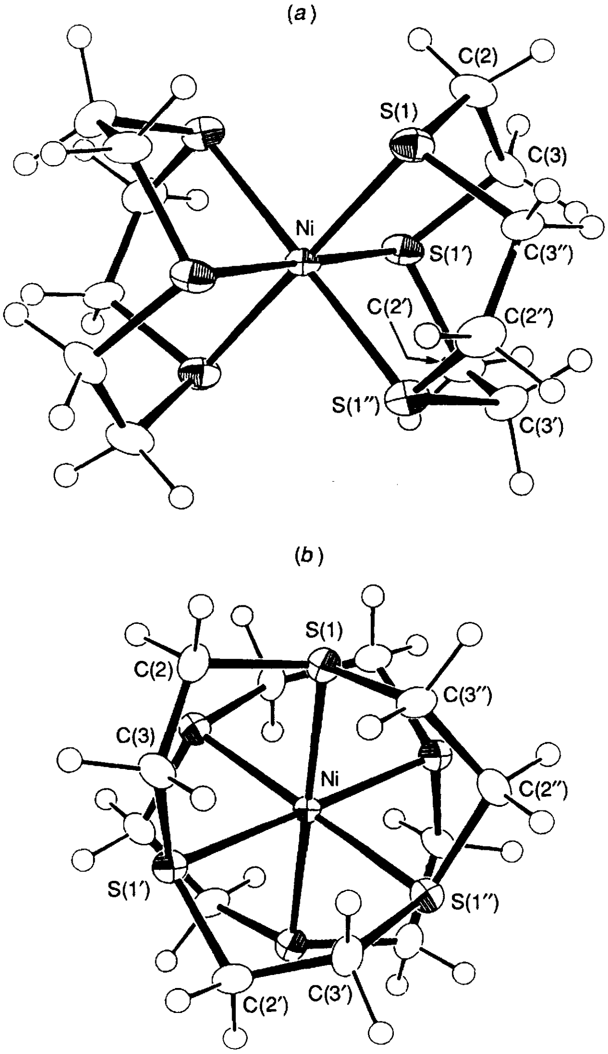

Fig. 3 Two views of the structure of $[Ni([9]aneS_3)_2]^{3+}$ with the numbering scheme adopted

This is consistent with the removal of an electron from a formally Ni–S antibonding $e_g{}^*$ orbital on oxidation of Ni^{II} to Ni^{III}. The high symmetry found for $[Ni([9]aneS_3)_2]^{3+}$ in the crystal is not consistent with the rhombic symmetry of the ESR spectra observed for this species, implying that the expected axis of Jahn–Teller distortion for the d^7 nickel(III) centre may be statistically disordered about a three-fold axis. The analogous complexes $[Ni([9]aneN_3)_2]^{3+}$ [Ni–N = 1.964(5), 1.970(5), 2.107(5) Å[15]] and $[Pd([9]aneS_3)_2]^{3+}$, [Pd–S = 2.3558(14), 2.3692(15), 2.5448(15) Å[9]] both exhibit a Jahn–Teller elongation in the solid state. However, despite the presence of disorder, the X-ray structural determination confirms the oxidation to have occurred predominantly at the metal centre rather than at the S-donor site(s). If the latter were the case, the Ni–S distances in the $[Ni([9]aneS_3)_2]^{3+}$ cation would be expected to be longer than in $[Ni([9]aneS_3)_2]^{2+}$ due to repulsion between Ni^{II} and the S-based radical cation. To our knowledge, $[Ni([9]aneS_3)_2]^{3+}$ represents the first structurally characterised nickel(III) complex incorporating thioether donors. Attempts to crystallise the $[Ni([9]aneS_3)_2]^{3+}$ cation with other counter ions have been unsuccessful thus far due to the relative instability of the 3+ cation.

The reductive electrochemistry of $[Ni([9]aneS_3)_2]^{2+}$ was also investigated. Controlled-potential electrolysis of $[Ni([9]aneS_3)_2][PF_6]_2$ in MeCN containing 0.1 mol dm^{-3} NBu_4PF_6 at −1.00 V *vs.* Ag–AgCl at 293 or 253 K affords pale green solutions, together with some deposition of Ni metal onto the Pt working electrode. These solutions exhibit complex ESR spectra, which appear to contain peaks from more than one paramagnetic product, although signals at $g_\perp = 2.055$, $g_\parallel = 2.175$ are tentatively assigned to an intermediate nickel(I) species. Coulometric determinations of this process at 253 K consistently gave values between 1 and 2 electrons per Ni, typically $n \approx 1.4$ electrons, also implying decomposition of the initial reduction product. These results are consistent with the formation of the highly reactive $[Ni([9]aneS_3)_2]^{+}$ which then decomposes, possibly by disproportionation to $[Ni([9]aneS_3)_2]^{2+}$ and Ni metal, or by loss of one or more $[9]aneS_3$ ligands. The analogous complex $[Ni([9]aneNS_2)_2]^{2+}$ has been shown to form tetrahedral $[Ni([9]aneNS_2)L]^{+}$ (L = NCMe or PPh_3) on reduction, *via* loss of one macrocyclic ligand.[16]

In order to investigate the possibility of generating a metal-stabilised $[9]aneS_3$-radical cation about a redox-inactive metal centre, the electrochemistry of the octahedral complex $[Zn([9]aneS_3)_2]^{2+}$[22] was also examined. $[Zn([9]aneS_3)_2][PF_6]_2$ was prepared by the reaction of $Zn(NO_3)_2{\cdot}6H_2O$ with 2 molar equivalents of $[9]aneS_3$ in MeCN at 293 K, followed by counter ion metathesis with NH_4PF_6. Cyclic voltammetry of $[Zn([9]aneS_3)_2][PF_6]_2$ in MeCN containing 0.1 mol dm^{-3} NBu_4PF_6 at 293 K shows an irreversible oxidation at E_{pa} = +1.30 V (scan rate 400 mV s^{-1}) and an irreversible reduction at E_{pc} = −1.77 V, together with an associated desorption spike at E_{pa} = −0.60 V due to deposition of Zn metal onto the Pt working electrode. These processes remain irreversible at scan rates up to 1100 mV s^{-1} at 273 K, showing that any oxidised or reduced products from this compound are extremely unstable.

The results described herein suggest that the one-electron oxidation product of $[Ni([9]aneS_3)_2]^{2+}$ can be regarded as predominantly a metal-based d^7 nickel(III) radical species which has been characterised spectroelectrochemically by ESR and electronic spectroscopy, and crystallographically. The stabilisation of d^7 radical species by homoleptic thioether co-ordination is now established, and reflects the co-ordinative and electronic flexibility of these types of ligands.

Experimental

Infrared spectra were run as KBr discs using a Perkin Elmer 598 spectrometer over the range 200–4000 cm^{-1}. Fast-atom bombardment mass spectra were obtained on a Kratos MS 50TC spectrometer using a 3-nitrobenzyl alcohol (noba) matrix. Microanalyses were performed by the Edinburgh University Chemistry Department Microanalytical Service. Proton NMR spectra were run on a Bruker WH80 spectrometer operating at 80.13 MHz. ESR spectra were run as mobile solutions or as frozen glasses down to 77 K using a Bruker ER200D spectrometer. Electrochemical measurements were performed using Bruker E310 and E130M modular polarographs. All readings were taken using a three-electrode potentiostatic system in MeCN containing 0.1 mol dm^{-3} NBu_4PF_6 as supporting electrolyte. Cyclic voltammetric measurements were carried out using a double platinum electrode and a Ag–AgCl reference electrode. All potentials are quoted *versus* ferrocene–ferrocenium. Electronic spectra were measured in 1 cm quartz cells using a Perkin Elmer Lambda 9 spectrophotometer. Spectroelectrochemical measurements were carried out in a quartz cell (path length 0.5 mm) fitted with a 0.35 mm platinum–rhodium gauze as a working electrode. The platinum auxiliary electrode and Ag–Ag$^+$ reference electrode were fitted into a quartz extension attached to the cell, and were protected from the bulk solution by porous glass frits. The temperature of the cell was maintained and controlled by the passage of dry, pre-cooled nitrogen gas around the assembly, and monitored using a thermocouple and digital thermometer.

1,4,7-Trithiacyclononane was purchased from Aldrich Chemicals. 62%-Enriched ^{61}Ni foil was purchased from the Atomic Energy Research Establishment, Harwell, and converted to $^{61}Ni(NO_3)_2{\cdot}6H_2O$ by dissolution in the minimum volume of 70% w/w HNO_3 followed by crystallisation at 253 K.

Synthesis of $[Ni([9]aneS_3)_2][PF_6]_2$.—Nickel(II) dichloride hexahydrate (0.059 g, 2.5 × 10^{-4} mol) and [9]aneS$_3$ (0.090 g, 5.0 × 10^{-4} mol) were allowed to react in refluxing MeOH (15 cm^3) for 1 h to afford a pink solution. Addition of NH_4PF_6 (0.082 g, 5.0 × 10^{-4} mol) and further refluxing for 30 min gave a pink precipitate, which was collected and recrystallised from MeCN–Et$_2$O. Yield 0.15 g, 82% (Found: C, 20.4; H, 3.4. Calc. for $C_{12}H_{24}F_{12}NiP_2S_6$: C, 20.3; H, 3.4%). IR spectrum: 3000, 2940, 1445, 1415, 1300, 1285, 1255, 1180, 1140, 1010, 985, 930, 900, 840, 740, 690, 670, 635, 620, 555, 480 and 435 cm^{-1}. Electronic spectrum (in MeCN): λ_{max} 785 (ε_{max} = 37), 529 (36) and 319 nm (17 270 dm^3 mol^{-1} cm^{-1}). FAB mass spectrum (noba): found: *m*/*z* 562, 418; calc. for $[^{58}Ni([9]aneS_3)([9]aneS_3 - H)(PF_6)]^+$ 562, $[^{58}Ni([9]aneS_3)_2]^+$ 418 with correct isotopic distribution.

Synthesis of $[^{61}Ni([9]aneS_3)_2][PF_6]_2$.—Method as above, using $^{61}Ni(NO_3)_2{\cdot}6H_2O$ (62%-enriched, 0.041 g, 1.4 × 10^{-4} mol) with appropriate reductions in the other reactants and solvents. Yield 0.70 g, 70% (Found: C, 20.5; H, 3.5. Calc. for $C_{12}H_{24}F_{12}NiP_2S_6$: C, 20.3; H, 3.4%).

Synthesis of $[Zn([9]aneS_3)_2][PF_6]_2$.[22]—Zinc nitrate hexahydrate (0.050 g, 1.7 × 10^{-4} mol) and [9]aneS$_3$ (0.060 g, 3.4 × 10^{-4} mol) were stirred in MeCN (10 cm^3) at 293 K for 1 h giving a white precipitate. Ammonium hexafluorophosphate (0.052 g, 3.4 × 10^{-4} mol) was added, and the mixture stirred for a further 1 h. The resultant colourless solution was filtered, reduced to one-third of its original volume, and the white microcrystalline complex precipitated by addition of Et$_2$O. The complex was recrystallised from MeNO$_2$–Et$_2$O. Yield 0.093 g, 78% (Found: C, 20.0; H, 3.5. Calc. for $C_{12}H_{24}F_{12}P_2S_6Zn$: C, 20.1; H, 3.4%). IR spectrum: 2960, 2920, 2900, 2800, 1450, 1410, 1380, 1300, 1285, 1255, 1220, 1190, 1155, 1135, 1100, 940, 840, 775, 700, 670, 655, 615, 555, 475 and 430 cm^{-1}. FAB mass spectrum: found: *m*/*z* 569, 423 and 243; calc. for $[^{64}Zn([9]aneS_3)_2(PF_6)]^+$ 569, $[^{64}Zn([9]aneS_3)([9]aneS_3 - H)]^+$ 423, $[^{64}Zn([9]aneS_3 - H)]^+$ 243 with correct isotopic distribution. Proton NMR spectrum (CD$_3$CN, 293 K, 80.13 MHz): δ 3.09 (br, [9]aneS$_3$, SCH$_2$).

Single-crystal X-Ray Structure of $[Ni([9]aneS_3)_2][H_5O_2]_3[ClO_4]_6$.—Crystals were grown in 70% perchloric acid, coated in a film of Nujol for protection and transferred into a Lindemann glass capillary tube: this was then mounted on a Stoë STADI-4 four-circle diffractometer equipped with an Oxford Cryosystems low-temperature device.[23] Throughout this transfer procedure the crystals were cooled using solid carbon dioxide.

Table 1 Bond lengths (Å), angles and torsions angles (°) for the complex $[Ni^{III}([9]aneS_3)_2][H_5O_2]_3[ClO_4]_6$ with estimated standard deviations (e.s.d.s) in parentheses *

Ni–S(1)	2.3129(25)	S(1)–C(3″)	1.820(11)
S(1)–C(2)	1.813(10)	C(2)–C(3)	1.533(17)
Cl–O(1)	1.444(12)	Cl–O(2)	1.436(11)
Cl–O(3)	1.401(13)	Cl–O(4)	1.373(14)
S(1)–Ni–S(1′)	90.31(25)	C(2)–S(1)–C(3″)	102.8(5)
Ni–S(1)–C(2)	100.0(3)	S(1)–C(2)–C(3)	113.8(8)
Ni–S(1)–C(3″)	103.6(3)	S(1′)–C(3)–C(2)	111.2(9)
O(1)–Cl–O(2)	109.8(6)	O(2)–Cl–O(3)	109.7(7)
O(1)–Cl–O(3)	106.7(7)	O(2)–Cl–O(4)	108.8(7)
O(1)–Cl–O(4)	112.6(8)	O(3)–Cl–O(4)	109.3(8)
C(3″)–S(1)–C(2)–C(3)	61.9(9)		
S(1)–C(2)–C(3)–S(1′)	52.4(11)		
C(2)–C(3)–S(1′)–C(2′)	−30.6(10)		

* Singly and doubly primed atoms are related to their unprimed equivalents by the symmetry operations (1 − *y*, 1 + *x* − *y*, *z*) and (*y* − *x*, 1 − *x*, *z*) respectively.

Table 2 Atomic coordinates for $[Ni^{III}([9]aneS_3)_2][H_5O_2]_3[ClO_4]_6$ with e.s.d.s in parentheses

Atom	*x*	*y*	*z*
Ni	0.333 33	0.666 67	0.166 67
S(1)	0.450 84(17)	0.651 58(17)	0.122 35(8)
C(2)	0.511 2(7)	0.775 6(7)	0.095 0(3)
C(3)	0.435 2(7)	0.807 7(7)	0.078 2(3)
Cl	0.717 62(21)	0.717 32(24)	0.174 02(11)
O(1)	0.654 6(7)	0.611 4(7)	0.187 1(4)
O(2)	0.664 1(7)	0.772 1(7)	0.182 6(3)
O(3)	0.735 3(9)	0.717 4(8)	0.128 1(4)
O(4)	0.809 9(8)	0.765 3(10)	0.196 1(4)
O(1W)	0.633 8(9)	0.475 0(10)	0.119 8(4)

Crystal data. $C_{12}H_{24}NiS_6{}^{3+}{\cdot}3H_5O_2{}^+{\cdot}6ClO_4{}^-$, *M* = 1127.05, rhombohedral, space group $R\bar{3}c$, *a* = 15.060(4), *c* = 29.966(12) Å, *U* = 5886 Å^3 [from 2θ values of 42 reflections measured at ±ω (2θ = 24–26°, $\bar{\lambda}$ = 0.710 73 Å)], *Z* = 6, D_c = 1.908 g cm^{-3}, *T* = 173 ± 0.1 K, deep red equant crystal, 0.69 × 0.58 × 0.58 mm, μ = 1.310 mm^{-1}, *F*(000) = 3462.

Data collection and processing. STADI-4 diffractometer, graphite-monochromated Mo-Kα X-radiation, *T* = 173 K, ω–2θ scans with ω width given by (1.40 + 0.347 tan θ)°, 1003 data collected ($2\theta_{max}$ 45°, *h* −11 to 0, *k* 0–16, *l* 0–32), 909 unique (R_{int} 0.074), giving 722 reflections (*n*) with $F \geqslant 6\sigma(F)$ for use in all calculations. The intensities of three standard reflections varied by ≤ ±4% during the course of the data collection.

Structure solution and refinement. With the nickel atom placed on the origin, iterative cycles of least-squares refinement and Fourier difference synthesis located all non-H atoms.[24] At isotropic convergence, final corrections (minimum 1.253, maximum 1.624) for absorption were applied using DIFABS.[25] Non-H atoms were then refined (by least squares on *F*)[24] with anisotropic thermal parameters, with the macrocyclic H atoms included at fixed, calculated positions. The H atoms of $HClO_4$ and $H_5O_2{}^+$ were not located. At final convergence $R\ (= \Sigma||F_o| - |F_c||/\Sigma F_o)$, $R'\ [= \Sigma w(|F_o| - |F_c|)^2/\Sigma w|F_o|^2)^{\frac{1}{2}}]$ = 0.0745, 0.0884 respectively, $S\ \{= [\Sigma w(|F_o| - |F_c|)^2/(n - p)]^{\frac{1}{2}}\}$ = 1.202 for 91 refined parameters (*p*) and the final Δ*F* synthesis showed no Δρ above 1.10 or below −0.57 e Å^{-3}. A secondary extinction parameter refined to 1.9(5) × 10^{-8}, the weighting scheme $w^{-1} = \sigma^2(F) + 0.000\,122F^2$ gave satisfactory agreement analyses and in the final cycle $(\Delta/\sigma)_{max}$ was 0.50.

Table 1 gives bond lengths, angles and torsions, while atomic coordinates appear in Table 2.

The $[Ni([9]aneS_3)_2]^{3+}$ ion has crystallographically imposed $\bar{3}$ (S_6) symmetry and shows no signs of disorder. The ClO_4^- ion has no imposed symmetry and refines satisfactorily as a single ordered group. The atom O(1W) is located 2.35(3) Å from an atom related to it by the two-fold axis at $\frac{2}{3}, y, \frac{1}{12}$ indicating a strong, possibly symmetric hydrogen bond. Atom O(1W) also has short contacts of 2.78(2) Å with O(1) and 2.87(2) Å with O(2) at $y - \frac{1}{3}, \frac{1}{3} - x + y, \frac{1}{3} - z$. These indicate the presence of other hydrogen bonds, and are only compatible with the presence of an $H_5O_2^+$ astride the two-fold axis. The unit-cell charge is thus balanced, as it contains 6 $[Ni([9]aneS_3)_2]^{3+}$ ions, 18 $H_5O_2^+$ ions and 36 ClO_4^- ions.

Atomic scattering factors were inlaid,[24] or taken from ref. 26. Molecular geometry calculations utilised CALC[27] and Fig. 3 was produced with ORTEPII.[28]

Acknowledgements

We thank ICI Colours and Fine Chemicals (Blackley) for a CASE Awards (to M. A. H.), the SERC for support, and the Royal Society of Edinburgh and Scottish Office Education Department for a Support Research Fellowship (to M. S.).

References

1 S. W. Ragsdale, L. G. Ljungdahl and D. V. DerVartanian, *Biochem. Biophys. Res. Commun.*, 1982, **108**, 658; 1983, **115**, 658; P. A. Lindahl, N. Kojima, R. P. Hausinger, J. A. Fox, B. K. Teo, C. T. Walsh and W. H. Orme-Johnson, *J. Am. Chem. Soc.*, 1984, **106**, 3062; R. A. Scott, S. A. Wallin, M. Czechowski, D. V. DerVartanian, J. LeGall, H. D. Peck, jun. and I. Moura, *J. Am. Chem. Soc.*, 1984, **106**, 6864; V. M. Fernandez, E. C. Hatchikian, D. S. Patil and R. Cammack, *Biochim. Biophys. Acta*, 1986, **883**, 145; R. Cammack, *Adv. Inorg. Chem.*, 1988, **32**, 297.

2 H.-J. Krüger and R. H. Holm, *Inorg. Chem.*, 1989, **28**, 1148; M. Kumar, R. O. Day, G. J. Colpas and M. J. Maroney, *J. Am. Chem. Soc.*, 1989, **111**, 5974.

3 H.-J. Krüger and R. H. Holm, *Inorg. Chem.*, 1987, **26**, 3645; *J. Am. Chem. Soc.*, 1990, **112**, 2955; S. Fox, Y. Wang, A. Silver and M. Millar, *J. Am. Chem. Soc.*, 1990, **112**, 3218; S. B. Choudhury, D. Ray and A. Chakravorty, *Inorg. Chem.*, 1990, **29**, 4603; 1991, **30**, 4354; H.-J. Krüger, G. Peng and R. H. Holm, *Inorg. Chem.*, 1991, **30**, 734.

4 M. Zimmer, G. Schulte, X.-L. Luo and R. H. Crabtree, *Angew. Chem., Int. Ed. Engl.*, 1991, **30**, 193; P. Stavropoulos, M. C. Muetterties, M. Carrié and R. H. Holm, *J. Am. Chem. Soc.*, 1991, **113**, 8485.

5 W. N. Setzer, C. A. Ogle, G. S. Wilson and R. S. Glass, *Inorg. Chem.*, 1983, **22**, 266.

6 K. Wieghardt, H.-J. Küppers and J. Weiss, *Inorg. Chem.*, 1985, **24**, 3067.

7 M. Schröder, *Pure Appl. Chem.*, 1988, **60**, 517; A. J. Blake and M. Schröder, *Adv. Inorg. Chem.*, 1990, **35**, 1; G. Reid and M. Schröder, *Chem. Soc. Rev.*, 1990, **19**, 239.

8 A. J. Blake, A. J. Holder, T. I. Hyde, Y. V. Roberts, A. J. Lavery and M. Schröder, *J. Organomet. Chem.*, 1987, **323**, 261; see also K. Wieghardt, H.-J. Küppers, E. Raabe and C. Krüger, *Angew. Chem., Int. Ed. Engl.*, 1986, **25**, 1101.

9 A. J. Blake, A. J. Holder, T. I. Hyde and M. Schröder, *J. Chem. Soc., Chem. Commun.*, 1987, 987.

10 A. J. Blake, R. O. Gould, A. J. Holder, T. I. Hyde, A. J. Lavery, M. O. Odulate and M. Schröder, *J. Chem. Soc., Chem. Commun.*, 1987, 118.

11 S. C. Rawle, R. Yagbasan, K. Prout and S. R. Cooper, *J. Am. Chem. Soc.*, 1987, **109**, 6181; A. J. Blake, R. O. Gould, A. J. Holder, T. I. Hyde and M. Schröder, *J. Chem. Soc., Dalton Trans.*, 1988, 1861; S. R. Cooper, S. C. Rawle, R. Yagbasan and D. J. Watkin, *J. Am. Chem. Soc.*, 1991, **113**, 1600.

12 A. J. Blake, A. J. Holder, A. Taylor and M. Schröder, *New J. Chem.*, 1991, **15**, 511.

13 K. Nag and A. Chakravorty, *Coord. Chem. Rev.*, 1980, **33**, 87; A. G. Lappin and A. McAuley, *Adv. Inorg. Chem.*, 1988, **32**, 241.

14 A. McAuley, P. R. Norman and O. Olubuyide, *Inorg. Chem.*, 1984, **23**, 1684.

15 K. Wieghardt, W. Walz, J. Bordner, B. Nuber, J. Weiss, A. Ozarowski, H. Stratemeier and D. Reinen, *Inorg. Chem.*, 1986, **25**, 1650.

16 L. Fabbrizzi and D. M. Proserpio, *J. Chem. Soc., Dalton Trans.*, 1989, 229; A. McAuley and S. Subramanian, *Inorg. Chem.*, 1990, **29**, 2830; S. Chandrasekhar and A. McAuley, *Inorg. Chem.*, 1992, **31**, 480.

17 A. H. Maki, N. Edelstein, A. Davison and R. H. Holm, *J. Am. Chem. Soc.*, 1964, **86**, 4580; G. A. Bowmaker, P. D. W. Boyd, G. K. Campbell, H. M. Hope and R. L. Martin, *Inorg. Chem.*, 1982, **21**, 1152.

18 B. A. Goodman and R. B. Raynor, *Adv. Inorg. Chem. Radiochem.*, 1970, **13**, 135.

19 R. Kirmse, J. Stach, W. Dietzsch, G. Steimecke and E. Hoyer, *Inorg. Chem.*, 1980, **19**, 2679; C. T. Vance, R. D. Bereman, J. Bordner, W. E. Hatfield and J. H. Helms, *Inorg. Chem.*, 1985, **24**, 2679.

20 E. Balasivasubramanian, C. N. Sethulekshmi and P. T. Manoharan, *Inorg. Chem.*, 1982, **21**, 1684.

21 A. J. Blake, A. J. Holder, T. I. Hyde, H.-J. Küppers, M. Schröder, S. Stötzel and K. Wieghardt, *J. Chem. Soc., Chem. Commun.*, 1989, 1600.

22 H.-J. Küppers, K. Wieghardt, B. Nuber and J. Weiss, *Z. Anorg. Allg. Chem.*, 1989, **577**, 155.

23 J. Cosier and A. M. Glazer, *J. Appl. Crystallogr.*, 1986, **19**, 105.

24 G. M. Sheldrick, SHELX76, Program for Crystal Structure Determination, University of Cambridge, 1976.

25 N. Walker and D. Stuart, DIFABS, Program for empirical absorption corrections, *Acta Crystallogr., Sect. A*, 1983, **39**, 158.

26 D. T. Cromer and J. B. Mann, *Acta Crystallogr., Sect. A*, 1968, **24**, 321.

27 R. O. Gould and P. Taylor, CALC, Fortran 77 version, University of Edinburgh, 1985.

28 P. D. Mallinson and K. W. Muir, ORTEP II, interactive version, *J. Appl. Crystallogr.*, 1985, **15**, 51.

Received 2nd June 1992; *Paper* 2/02901D